

Twist-bend coupling, twist waves and the shape of DNA loops

SK. Nih^{1,2} M. Ch^{1,3} M. Lm^{1,3} K. Pp¹ E. P¹ dE. Ch¹

¹Laboratory for Soft Matter and Biophysics, KU Leuven, Celestijnenlaan 200D, 3001 Leuven, Belgium

²Flemish Institute for Technological Research (VITO), Boeretang 200, B-2400 Mol, Belgium

³Institut für Theoretische Physik, Universität Innsbruck, Technikerstraße 21A, A-6020 Innsbruck, Austria

(Dated: August 8, 2019)

By combining analytical and numerical calculations, we investigate the minimal-energy shape of short DNA loops of approximately 100 base pairs (bp). We show that in these loops the excess twist density oscillates as a response to an imposed bending stress, as recently found in DNA minicircles and observed in nucleosomal DNA. These twisted oscillations, here referred to as twist waves, are due to the coupling between twist and bending deformations, which in turn originates from the asymmetry between DNA major and minor grooves. We introduce a simple analytical variational shape, that reproduces the exact loop energy up to the fourth significant digit, and is in very good agreement with shapes obtained from coarse-grained simulations. We, finally, analyze the loop dynamics at room temperature, and show that the twist waves are robust against thermal fluctuations. They perform a normal diffusive motion, whose origin is briefly discussed.

I. INTRODUCTION

DNA

of approximately

100 base pairs (bp)

is investigated

analytically and

numerically

to determine the

minimal-energy

shape of short

DNA loops

of approximately

100 base pairs

(bp). We show

that in these

loops the excess

twist density

oscillates as a

response to an

imposed bending

stress, as recently

found in DNA

minicircles and

observed in

nucleosomal DNA.

These twisted

oscillations, here

referred to as

twist waves, are

due to the

coupling between

twist and bending

deformations,

which in turn

originates from

the asymmetry

between DNA

major and minor

grooves. We

introduce a

simple analytical

variational shape,

that reproduces

l_b , l_p

[8] and

DNA

of

approximately

100 base pairs

(bp). We

show that in

these loops the

excess twist

density oscillates

as a response

to an imposed

bending stress,

as recently

found in DNA

minicircles

and observed in

nucleosomal DNA.

These twisted

oscillations, here

referred to as

twist waves, are

due to the

coupling between

twist and bending

deformations,

which in turn

originates from

the asymmetry

between DNA

major and minor

grooves. We

introduce a

simple analytical

variational shape,

that reproduces

the exact loop

energy up to the

fourth significant

digit, and is in

very good

agreement with

shapes obtained

from coarse-grained

II. DNA ELASTICITY AND TWIST-BEND COUPLING

DNA is modeled

as a

rod of length L

with fixed ends

at $s=0$ and $s=L$

and

$$\beta E = \frac{l_b}{2} \int_0^L ds \left(\frac{d\hat{e}_3}{ds} \right)^2, \quad (1)$$

where $\beta = 1/k_B T$

is the inverse

thermal energy

and $\hat{e}_1, \hat{e}_2, \hat{e}_3$

are the unit

vectors along the

rod axis.

In DNA, the

twist is

described by

the angle θ

around the

rod axis.

The twist

density is

defined as

$\tau = \frac{1}{l_p} \frac{d\theta}{ds}$

and the

twist energy

is

$E_{\text{twist}} = \frac{1}{2} \int_0^L ds l_p \tau^2$

where

l_p is the

\leq

l_b is

$\{\hat{e}_1, \hat{e}_2, \hat{e}_3\}$

\hat{e}_1 and \hat{e}_2

\hat{e}_3 is

\hat{e}_2

\hat{e}_1

$\{\hat{e}_1, \hat{e}_2, \hat{e}_3\}$ in s

$s+ds$

$$\frac{d\hat{e}_i}{ds} = (\Omega + \omega_0 \hat{e}_3) \times \hat{e}_i, \quad (2)$$

where $i = 1, 2, 3$ and $\omega_0 \approx 1.75$

is the

twist

wave

number

per

base

pair.

if $\Omega = 0$ (i.e., $\hat{e}_3 = \mathbf{n}$), in \hat{e}_1 and \hat{e}_2 are $\hat{e}_1 = \frac{\omega_0}{\Omega} \mathbf{e}_1$ and $\hat{e}_2 = \frac{\omega_0}{\Omega} \mathbf{e}_2$. Here $\Omega = \omega_0 \sqrt{1 - \frac{v^2}{c^2}}$ is the relativistic frequency, \mathbf{e}_i are the Cartesian unit vectors, and \mathbf{n} is the unit vector along the DNA helix axis [5].

$$\beta E = \frac{1}{2} \int_0^L ds (A_1 \Omega_1^2 + A_2 \Omega_2^2 + C \Omega_3^2 + 2G \Omega_2 \Omega_3). \quad (3)$$

Here A_1 and A_2 are the bending stiffnesses, C is the torsional stiffness, G is the coupling between the bending and torsional modes, and Ω_i are the components of the unit vector $\hat{\Omega}$ in the Cartesian basis. Note that Eq. (2) can be written as

$$\kappa^2 \equiv \left(\frac{d\hat{e}_3}{ds} \right)^2 = \Omega_1^2 + \Omega_2^2, \quad (4)$$

where κ is the curvature. For $A_1 = A_2 = l_b$, $C = 0$, and $G = 0$, Eq. (3) reduces to the standard worm-like chain model [6]. In the case of a DNA helix, $A_1 \neq A_2$ and $G \neq 0$ is

$$\begin{aligned} \Omega_1 &= \frac{l_b}{A_1} \frac{\omega_0 s}{R}, \\ \Omega_2 &= \frac{l_b}{\tilde{A}_2} \frac{\omega_0 s}{R}, \\ \Omega_3 &= -\frac{G}{C} \Omega_2, \end{aligned} \quad (5)$$

where R is the radius

$$\tilde{A}_2 = A_2 \left(1 - \frac{G^2}{A_2 C} \right), \quad (6)$$

and l_b is the persistence length [3].

$$\frac{1}{l_b} = \frac{1}{2} \left(\frac{1}{A_1} + \frac{1}{\tilde{A}_2} \right), \quad (7)$$

ie, $\frac{1}{l_b} = \frac{1}{2} \left(\frac{1}{A_1} + \frac{1}{\tilde{A}_2} \right)$ [6]. Here Ω_1 and Ω_2 are the components of the unit vector $\hat{\Omega}$ in the Cartesian basis, and Ω_3 is the component along the DNA helix axis. Note that Eq. (5) can be written as $\Omega_1 = \frac{l_b}{A_1} \frac{\omega_0 s}{R}$ and $\Omega_2 = \frac{l_b}{\tilde{A}_2} \frac{\omega_0 s}{R}$ [20].

III. HARMONIC LOOPS IN THE WLC MODEL

Consider a DNA helix of length L [14]. According to [21], the harmonic loop model (HLM) [Eq. (1)] can be used to describe the DNA helix. The HLM is a simple model for the DNA helix, where the DNA helix is represented by a chain of spheres (beads) connected by springs. The DNA helix is assumed to be in equilibrium with a force F applied at one end. The HLM is a simple model for the DNA helix, where the DNA helix is represented by a chain of spheres (beads) connected by springs. The DNA helix is assumed to be in equilibrium with a force F applied at one end. The HLM is a simple model for the DNA helix, where the DNA helix is represented by a chain of spheres (beads) connected by springs. The DNA helix is assumed to be in equilibrium with a force F applied at one end.

As shown in

$$\hat{e}_3 = \cos \theta \hat{x} + \sin \theta \hat{y}, \quad (8)$$

where \hat{x} and \hat{y} are the Cartesian unit vectors, and $\kappa = |d\theta/ds|$ [Eq. (4)] is the curvature.

$$\frac{d\theta(0)}{ds} = \frac{d\theta(L)}{ds} = 0. \quad (9)$$

A simple

$$\frac{d\theta^{(1)}}{ds} = \frac{\pi c_1}{L} \sin \left(\frac{\pi s}{L} \right), \quad (10)$$

where c_1 is the

$$J_0(c_1) = 0,$$

where J_0 is the Bessel function of the first kind.

Eq. (B3) [21] can be written as $J_0(c_1) = 0$, where $c_1 = 2.40482556$.

Fig. 1(a) shows the

Eq. (10), where

Eq. (8) can be written as

Fig. 1(b) shows Eq. (10), where L is the length of the DNA helix.

As shown in

IV. MINIMAL-ENERGY CONFIGURATION OF DNA LOOPS: MODULATED TWIST WAVES

A. Analytical results

From Eq (16) and Eq (5), we have

$$\begin{aligned} \Omega_1^{(1)} &= \frac{l_b}{A_1} \frac{\pi c_1}{L} \sin\left(\frac{\pi s}{L}\right) \sin(\omega_0 s + \phi), \\ \Omega_2^{(1)} &= \frac{l_b}{\tilde{A}_2} \frac{\pi c_1}{L} \sin\left(\frac{\pi s}{L}\right) \cos(\omega_0 s + \phi), \\ \Omega_3^{(1)} &= -\frac{G}{C} \Omega_2^{(1)}, \end{aligned} \quad (17)$$

From Eq (5) and Eq (12), we have

$$\begin{aligned} \Omega_1^{(3)} &= \frac{l_b}{A_1} \frac{\pi}{L} \left[c_1 \sin\left(\frac{\pi s}{L}\right) + c_3 \sin\left(\frac{3\pi s}{L}\right) \right] \sin(\omega_0 s + \phi), \\ \Omega_2^{(3)} &= \frac{l_b}{\tilde{A}_2} \frac{\pi}{L} \left[c_1 \sin\left(\frac{\pi s}{L}\right) + c_3 \sin\left(\frac{3\pi s}{L}\right) \right] \cos(\omega_0 s + \phi), \\ \Omega_3^{(3)} &= -\frac{G}{C} \Omega_2^{(3)}. \end{aligned} \quad (18)$$

From Eq (5) and Eq (3), we have

$$\beta E_{\text{HL}}^{(1)} = \left(\frac{\pi c_1}{2}\right)^2 \frac{l_b}{L} + \beta \Delta E(\phi). \quad (19)$$

From Eq (11) and Eq (17), we have

$$\tilde{\kappa}_{\text{max}} \equiv \sqrt{\Omega_1^2 + \Omega_2^2} \Big|_{s=L/2}, \quad (20)$$

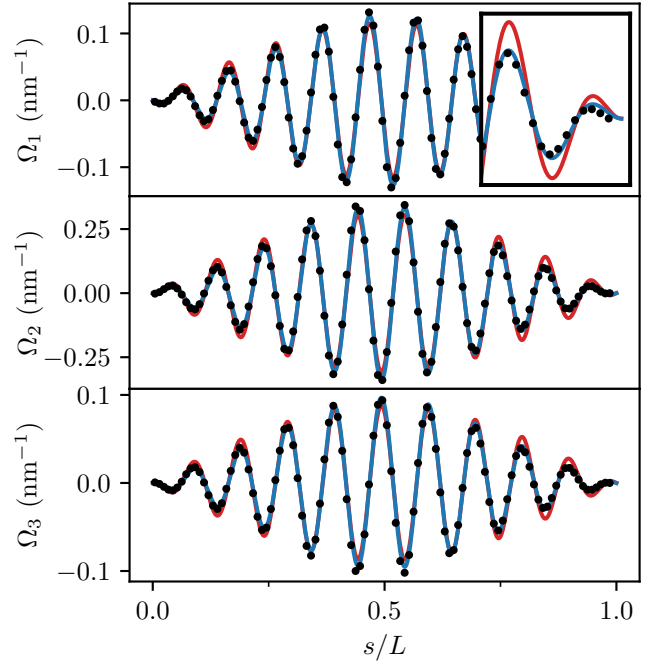


FIG. 2. Plots of the bending (Ω_1 and Ω_2) and twist (Ω_3) densities of a closed triad-model loop, as functions of the reduced arc-length s/L . The black circles are low-temperature Monte Carlo simulations of the triad model (with 104 bp), while the red and blue solid lines are the first- [Eq. (17)] and third-harmonic [Eq. (18)] ansatzes, respectively. The inset zooms into the one end of the loop, and reveals that the third-harmonic ansatz more accurately reproduces the data. The stiffness constants were chosen as $A_1 = 81$ nm, $A_2 = 39$ nm, $C = 105$ nm and $G = 30$ nm, calculated in Ref. [17] from the oxDNA2 model. The global phase $\phi = 4.02$ rad is the only fitting parameter.

From Eq (14) and Eq (18), we have

$$\frac{2\tilde{A}_2}{A_1 + \tilde{A}_2} \leq \frac{\tilde{\kappa}_{\text{max}}}{\kappa_{\text{max}}} \leq \frac{2A_1}{A_1 + \tilde{A}_2}, \quad (21)$$

From Eq (21) and Eq (17) and (18), we have

$$\tilde{\kappa}_{\text{max}} \leq \kappa_{\text{max}}.$$

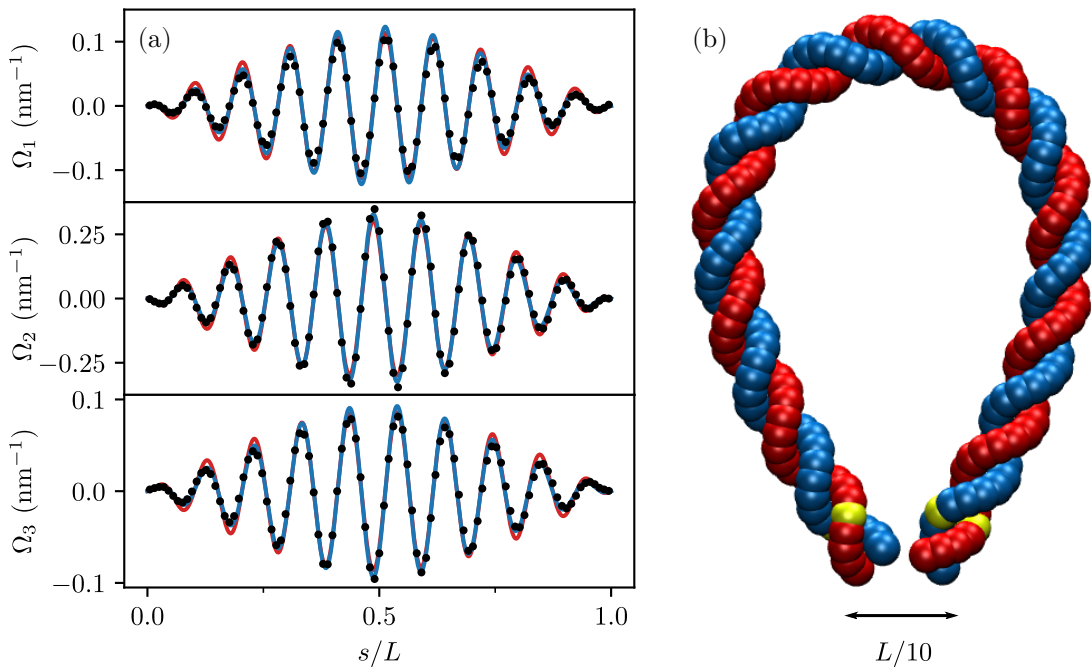


FIG. 3. (a) Similar to Fig. 2, but with the data obtained from low-temperature oxDNA2 simulations (black points). For the harmonic approximations [Eqs. (17) and (18), shown with red and blue lines, respectively] we used the same values as in Fig. 2, extracted from oxDNA2 simulations [17]. Once more, the global phase $\phi = 1.70$ rad is the only fitting parameter. (b) Actual configuration of the loop from which the plots in (a) were produced. The yellow points indicate the bp that were tethered to two fixed points in space by means of harmonic springs, effectively fixing the end distance (center-of-mass distance between the two pairs of yellow beads) at $d = L/10$.

B. Numerical analysis

In order to fit Eq (17) and (18), we

used the data from Fig 2, and Eq (3).

A DNA loop of length L is

described by

the set of

coordinates \mathbf{C}_i

and the set of

orientations \mathbf{e}_i .

The DNA is

assumed to be

in equilibrium

at $T = 1$ K (Fig 2).

The angular

velocities Ω_i

are given by

Eq (17) and

Eq (18).

The fitting

parameters are

A_1, A_2, C and

G .

The fitting

parameters are

c_1 and c_3 .

The fitting

parameters are

N beads

with

orientations $\{\hat{e}_1, \hat{e}_2, \hat{e}_3\}$, and

the global phase ϕ .

The fitting

parameters are

$a = 0.34$ nm

and $d = L/10$.

The fitting

parameters are

Ω_1, Ω_2 and

Ω_3 .

The fitting

parameters are

ϕ , A_1, A_2, C and

G .

The fitting

parameters are

c_1 and c_3 .

The fitting

parameters are

Ω_1, Ω_2 and

Ω_3 .

The fitting

parameters are

$a = 0.34$ nm

and $d = L/10$.

The fitting

parameters are

Ω_1, Ω_2 and

Ω_3 .

The fitting

parameters are

ϕ , A_1, A_2, C and

G .

The fitting

parameters are

c_1 and c_3 .

The fitting

parameters are

Ω_1, Ω_2 and

Ω_3 .

The fitting

parameters are

Ω_1, Ω_2 and

Ω_3 .

Fig 2). The fitting

parameters are

$|\Omega_3| \approx 0.1$ nm⁻¹, $\omega_0 = 1.75$ nm⁻¹, $\kappa_{\max} = 0.24$ nm⁻¹, $\tilde{\kappa}_{\max} = 0.34$ nm⁻¹, $T = 1$ K

and $\phi = 1.70$ rad.

The fitting

parameters are

Ω_1, Ω_2 and

Ω_3 .

The fitting

parameters are

ϕ, A_1, A_2, C and

G .

The fitting

parameters are

Ω_1, Ω_2 and

Ω_3 .

The fitting

parameters are

ϕ, A_1, A_2, C and

G .

The fitting

parameters are

c_1 and c_3 .

The fitting

parameters are

Ω_1, Ω_2 and

Ω_3 .

The fitting

parameters are

Ω_1, Ω_2 and

Ω_3 .

The fitting

parameters are

Ω_1, Ω_2 and

Ω_3 .

$\tilde{\kappa}_{\max} = 0.34$ nm⁻¹.

$T = 1$ K)

$d = L/10$

d

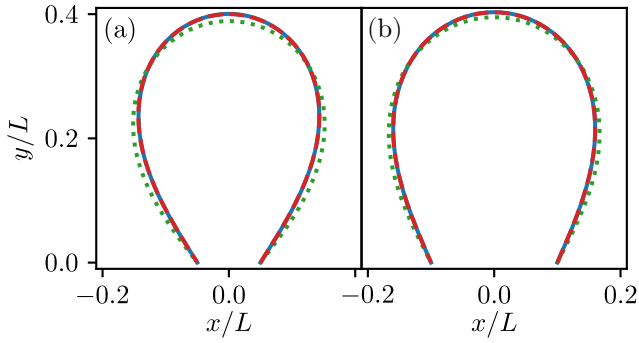


FIG. 6. Comparison of the shape among the one-harmonic approximation (10) (dotted green lines), two-harmonics approximation (12) (dashed red lines) and the exact solution (solid blue lines), with the two ends of the loop being fixed at a distance $L/10$ (a) and $L/5$ (b).

Appendix B: Harmonic loop ansatz

The ansatz is $\theta = \pi + \mu \phi$. As in the previous section, we assume the loop is fixed at $\theta = \pi$ at $x = 0$ and $x = L$.

$$U(\theta) = \mu \int_{\theta}^{\pi} \theta \approx \mu \left[-1 + \frac{(\theta - \pi)^2}{2} \right], \quad (\text{B1})$$

The boundary conditions are $\theta(0) = \theta(L) = \pi$.

$$\theta(L/2) = \pi + d.$$

$$\theta^{(1)}(s) = \pi - c_1 \sin\left(\frac{\pi s}{L}\right). \quad (\text{B2})$$

Nonlinearities are neglected in Eq(10). Plugging (A1), (B1) and (B2) into Eq(10), we get

$$\int_0^{\pi/2} \sin^2 \phi - c_1 \sin \phi d\phi \equiv \frac{\pi}{2} J_0(c_1) = 0, \quad (\text{B3})$$

where J_0 is the Bessel function of the first kind. The boundary conditions are $J_0(c_1) = 0$ and $J_0(c_3) = 0$.

$$J_0: c_1 = 2.4048.$$

$$\theta^{(3)}(s) = \pi - c_1 \sin\left(\frac{\pi s}{L}\right) - \frac{c_3}{3} \sin\left(\frac{3\pi s}{L}\right), \quad (\text{B4})$$

Plugging Eq(12), (B1) and (B4) into Eq(10), we get

$$\int_0^{\pi/2} \sin^2 \phi \left[c_1 \sin \phi + \frac{c_3}{3} \sin(3\phi) \right] d\phi = 0. \quad (\text{B5})$$

The boundary conditions are

$$J_0(c_1) = 0, \quad c_3 = 2.3703$$

$$J_0(c_3) = 0, \quad c_3 = -0.2808$$

The boundary conditions are

$$J_0(c_1) = 0, \quad c_3 = 2.3703$$

Using the boundary conditions (B2)

$$d(B4) = \frac{c_3}{3} \sin\left(\frac{3\pi}{2}\right)$$

$$E_3(B3) = d(B5) = -d/2L$$

(x = L/2) is the same as the

one in the previous section.

The results are shown in Fig 6.

a) $d = \frac{c_3}{3} \sin\left(\frac{3\pi}{2}\right) = -\frac{c_3}{3}$

b) $\theta = \pi$, $\theta(L) = \pi + d$

Using the boundary conditions

$$J_0(c_1) = 0, \quad c_3 = 2.3703$$

$$J_0(c_3) = 0, \quad c_3 = -0.2808$$

The results are shown in Fig 6.

Appendix C: Calculation of the energy

The energy is

$$E = \int_0^L \left[\frac{1}{2} \dot{\theta}^2 + U(\theta) \right] ds$$

Using the ansatz (B1) and (B2)

$$E = \int_0^L \left[\frac{1}{2} c_1^2 \sin^2\left(\frac{\pi s}{L}\right) + \mu \left(-1 + \frac{(\theta - \pi)^2}{2} \right) \right] ds$$

$$E = \int_0^L \left[\frac{1}{2} c_1^2 \sin^2\left(\frac{\pi s}{L}\right) + \mu \left(-1 + \frac{(\theta - \pi)^2}{2} \right) \right] ds$$

Using Eq(17), we get

$$E = \int_0^L \left[\frac{1}{2} c_1^2 \sin^2\left(\frac{\pi s}{L}\right) + \mu \left(-1 + \frac{(\theta - \pi)^2}{2} \right) \right] ds \quad (1)$$

$$\frac{1}{2} (A_1 \Omega_1^2 + A_2 \Omega_2^2 + C \Omega_3^2 + 2G \Omega_2 \Omega_3) = \frac{1}{2} (A_1 \Omega_1^2 + \tilde{A}_2 \Omega_2^2) = \left(\frac{l_b \pi c_1}{L} \right)^2 \int_0^L \left[\frac{\sin^2(\omega_0 s + \phi)}{2A_1} + \frac{\sin^2(\omega_0 s + \phi)}{2\tilde{A}_2} \right] ds \quad (\text{C1})$$

Using Eq(17) and the boundary conditions, we get

$$3. \quad \int_0^L \sin^2 \phi ds$$

Using the boundary conditions

$$A_2 = \frac{c_3^2}{3}$$

$$\tilde{A}_2 = \frac{c_3^2}{3}$$

$$4 \sin^2\left(\frac{\pi s}{L}\right) \sin^2(\omega_0 s + \phi) = 1 - \cos\left(\frac{2\pi s}{L} - \phi\right) \cos(\omega_0 s + 2\phi) + \frac{1}{2} \cos\left[2\left(\omega_0 - \frac{\pi}{L}\right)s + 2\phi\right] + \frac{1}{2} \cos\left[2\left(\omega_0 + \frac{\pi}{L}\right)s + 2\phi\right], \quad (\text{C2})$$

$$4 \sin^2\left(\frac{\pi s}{L}\right) \cos^2(\omega_0 s + \phi) = 1 - \cos\left(\frac{2\pi s}{L} + \phi\right) \cos(\omega_0 s + 2\phi) - \frac{1}{2} \cos\left[2\left(\omega_0 - \frac{\pi}{L}\right)s + 2\phi\right] - \frac{1}{2} \cos\left[2\left(\omega_0 + \frac{\pi}{L}\right)s + 2\phi\right], \quad (\text{C3})$$

Appendix

for $0 \leq s \leq L$.

Eq. (C2) and (C3) are Eq. (C1) and

Eq. (C3)

$\pi s/L$ and

Eq. (C2)

Eq. (C3), and

Eq. (C2) and (C3), and

Eq. (C2)

Eq. (C3)

Eq. (C2)

Eq. (C3) and

Eq. (C4) and Eq. (19) and

Eq. (19)

ϕ .

L , and

ϕ .

$$\beta E_{\text{HL}}^{(1)} = \frac{1}{2} \left(\frac{l_b \pi c_1}{L}\right)^2 \frac{L}{4} \left(\frac{1}{A_1} + \frac{1}{A_2}\right) + \beta \Delta E(\phi). \quad (\text{C4})$$

- [1] B. Alberts, D. Bray, J. Lewis, M. Raff, K. Roberts, and J. Watson, *Molecular Biology of the Cell*, 4th ed. (Garland, 2002).
- [2] A. Cournac and J. Plumbridge, *J. Bacteriol.* **195**, 1109 (2013).
- [3] I. Krivega and A. Dean, *Curr. Op. Gen. & dev.* **22**, 79 (2012).
- [4] A. Balaeff, L. Mahadevan, and K. Schulten, *Phys. Rev. Lett.* **83**, 4900 (1999).
- [5] I. Kulić and H. Schiessel, *Biophys. J.* **84**, 3197 (2003).
- [6] S. Sankararaman and J. F. Marko, *Phys. Rev. E* **71**, 021911 (2005).
- [7] Y. Zhang, A. E. McEwen, D. M. Crothers, and S. D. Levene, *Biophys. J.* **90**, 1903 (2006).
- [8] O.-c. Lee, J.-H. Jeon, and W. Sung, *Phys. Rev. E* **81**, 021906 (2010).
- [9] D. P. Wilson, A. V. Tkachenko, and J.-C. Meiners, *Europhys. Lett.* **89**, 58005 (2010).
- [10] A. G. Cherstvy, *J. Biol. Phys.* **37**, 227 (2011).
- [11] R. Vafabakhsh and T. Ha, *Science* **337**, 1097 (2012).
- [12] T. T. Le and H. D. Kim, *Nucleic Acids Res.* **42**, 10786 (2014).
- [13] Y.-J. Chen, S. Johnson, P. Mulligan, A. J. Spakowitz, and R. Phillips, *Proc. Natl. Acad. Sci. USA* **111**, 17396 (2014).
- [14] P. J. Mulligan, Y.-J. Chen, R. Phillips, and A. J. Spakowitz, *Biophys. J.* **109**, 618 (2015).
- [15] J. Marko and E. Siggia, *Macromolecules* **27**, 981 (1994).
- [16] S. K. Nomidis, F. Kriegel, W. Vanderlinden, J. Lipfert, and E. Carlon, *Phys. Rev. Lett.* **118**, 217801 (2017).
- [17] E. Skoruppa, M. Laleman, S. Nomidis, and E. Carlon, *J. Chem. Phys.* **146**, 214902 (2017).
- [18] E. Skoruppa, S. Nomidis, J. F. Marko, and E. Carlon, *Phys. Rev. Lett.* **121**, 088101 (2018).
- [19] S. K. Nomidis, E. Skoruppa, E. Carlon, and J. F. Marko, *Phys. Rev. E* **99**, 032414 (2019).
- [20] M. Caraglio, E. Skoruppa, and E. Carlon, *J. Chem. Phys.* **150**, 135101 (2019).
- [21] H. Yamakawa and W. Stockmayer, *J. Chem. Phys.* **57**, 2843 (1972).
- [22] T. E. Ouldridge, A. A. Louis, and J. P. Doye, *Phys. Rev. Lett.* **104**, 178101 (2010).
- [23] B. E. Snodin, F. Randisi, M. Mosayebi, P. Šulc, J. S. Schreck, F. Romano, T. E. Ouldridge, R. Tsukanov, E. Nir, and A. A. Louis, *J. Chem. Phys.* **142**, 234901 (2015).
- [24] S. Plimpton, *J. Comp. Phys.* **117**, 1 (1995).
- [25] O. Henrich, Y. A. G. Fosado, T. Curk, and T. E. Ouldridge, *Eur. Phys. J. E* **41**, 57 (2018).
- [26] The zeroth order Bessel function of the first kind has the following integral representation
- $$J_0(x) = \frac{1}{\pi} \int_0^\pi \cos(x \cos \phi) d\phi,$$
- see [27], p. 360.
- [27] M. Abramowitz and I. A. Stegun, *Mathematical functions with formulas, graphs, and mathematical tables* (National Bureau of Standards Applied Mathematics Series, Washington, 1972).